Silmaril: final design and on-sky performance

Cyprien Lanthermann[a], Theo ten Brummelaar[a], Peter Tuthill[b], Narsireddy Anugu[a], E. Robert Ligon[a], Gail Schaefer[a], Douglas Gies[c], Shashank Dholakia[d], and Adam Taras[b]

[a]The CHARA Array of Georgia State University, Mount Wilson Observatory, Mount Wilson, CA 91023, USA
[b]School of Physics, Sydney University, N.S.W. 2006, Australia
[c]Center for High Angular Resolution Astronomy and Department of Physics and Astronomy, Georgia State University, P.O. Box 5060, Atlanta, GA 30302-5060, USA
[d]School of Mathematics and Physics, University of Queensland, St Lucia, QLD 4072, Australia

ABSTRACT

Silmaril is a new 3-telescope beam combiner at the CHARA Array. In this presentation, we present the current design of the instrument, its on-sky measured and theoretical best performance, and its future development. Its design is specifically made to push for sensitivity. It combines 3 beams of the CHARA Array, allowing closure phase measurement but limiting the loss in sensitivity. It limits the number of optical elements to the minimum needed for combining the 3 beams. Using a CRED ONE camera allows for sub-electron readout noise, which means that our sensitivity is limited by the thermal background. Long focal-length cylindrical mirrors limit the thermal background by using an f/20 cold stop in front of the camera. We use a low spectral resolution prism to allow fringe tracking without compromising the instrument's sensitivity. Thanks to an ingenious edge filter design, we can observe both H- and K-band simultaneously, with a low thermal background on the H-band side of the detector. In the future, we intend to extend the instrument with a second set of 3 beams and add a Narcissus mirror to lower the thermal background and improve the sensitivity even more.

Keywords: e-APD, sensitivity, optical interferometry, near-infrared, K-band, H-band

1. INTRODUCTION

Optical Long Baseline Interferometry (OLBI) is known to be one of the most powerful observing techniques when it comes to angular resolution, only beaten by the Event Horizon Telescope which is an array of multiple radio telescope interferometers all over the globe.

The CHARA Array[1] is the OLBI facility with the best angular resolution power to date. It has baselines ranging from 34 to 331 m long, translating into an angular resolution of 0.7 mas in the K-band and 0.3 mas in the R-band. It is composed of six 1m-telescopes arranged in a Y shape. This disposition allows for a better UV-plane coverage, making the CHARA Array a great facility for interferometric image reconstruction.

The main issue with OLBI is its sensitivity. The most sensitive beam combiner at the CHARA Array is CLASSIC,[2] combining two telescopes and achieving a limiting magnitude of 8.5 in either H- or K-band. Recent developments have improved the sensitivity in the last decade. Examples of that are GRAVITY[3] at VLTI and MIRC-X[4,5] and MYSTIC[6,7] at the CHARA Array. The MIRC-X (H-band) and MYSTIC (K-band) instruments have a limiting magnitude of 7.5, getting close to CLASSIC and on par with CLIMB, the 3-telescope version of CLASSIC, while combing all six telescopes of the Array. This decreased the attractiveness and usefulness of CLASSIC and essentially made CLIMB obsolete. This motivated an upgrade to CLASSIC/CLIMB to focus on sensitivity; the project subsequently transformed into the new instrument Silmaril. We presented previously[8] the different elements of the design allowing for a better sensitivity, aiming for a gain in sensitivity of 2 magnitudes. This improvement in sensitivity will open the door for new science cases such as AGNs while expanding the current science cases already performed at the CHARA Array (stellar diameter measurement, binaries, disks

Further author information: (Send correspondence to C.L.)
C.L.: e-mail: clanthermann@gsu.edu

Optical and Infrared Interferometry and Imaging IX, edited by Jens Kammerer, Stephanie Sallum, Joel Sanchez-Bermudez, Proc. of SPIE Vol. 13095, 1309505
 · 0277-786X · doi: 10.1117/12.3012543

around YSOs, transient events, etc). In this proceeding, we summarize the previous design points in section 2, with an emphasis on parts that changed in the final design in sections 2.5 and 2.6. We then present the on-sky performance obtained with an engineering camera and the expected performance of the final design with the science camera in section 3 before concluding.

2. DESIGN KEY POINTS

The optical design of SILMARIL is focused on maximizing sensitivity while making as few compromises as possible in the other aspects of the instrument.

2.1 e-APD Detector

The main driver of the sensitivity gain for this instrument is the recent gain in performance of the e-APD detectors with the SAPHIRA detector that has been designed to be used in near-infrared interferometry and adaptive optics[9–12] in the GRAVITY instrument.[3] This detector is now integrated into a commercially available camera, the C-RED ONE,[13] manufactured by the First Light Imaging company recently acquired by Oxford Instruments. These cameras have since been implemented in several new beam combiners such as MIRC-X[4,5] and MYSTIC[6,7] at the CHARA Array. This camera has a fast readout (>1 kHz), a decent dark current, and a very low readout noise (<1 e^-/frame/pix) thanks to their electron avalanche process that amplifies the photon signal.

These characteristics are perfect for near-infrared interferometry that needs a faster read-out rate than the atmospheric turbulence timescale. Until recently the detectors used were limited by the readout noise. With the extremely low readout noise of the SAPHIRA detector, using them will make the instruments limited mostly by the thermal background noise. This involves a gain in sensitivity, which is the main goal of the Silmaril instrument. We chose to buy a C-RED ONE camera instead of building a camera ourselves with a SAPHIRA detector because the CHARA Array has already two of these cameras in use routinely in the MIRC-X and MYSTIC cameras. They have shown to be reliable and it will make the implementation of the Silmaril C-RED ONE camera easier as we can build our software[14] around the backbone of the software used for these working instruments.

2.2 3-Telescope Beam Combiner

To limit the loss in sensitivity caused by adding telescopes in a beam combiner instrument, we decided to limit Silmaril to 3 telescopes. Indeed, the experience of the CLASSIC and CLIMB instruments[2] shows that adding telescopes to combine their light in a beam combiner reduces the sensitivity of this instrument. CLASSIC is a 2-telescope beam combiner at the CHARA Array, and its limiting magnitude is 8.5. CLIMB is the 3 telescope version of the same instrument and has a limiting magnitude of 7. We decided to use 3 telescopes as it is the minimum number of telescopes required to measure the closure phase. To make use of the 6 telescopes of the CHARA Array, we plan to be able to replicate the 3-telescope design to combine twice 3 telescopes on the same detector, making Silmaril a 2×3 beam combiner. This will double the number of visibilities and closure phases measured simultaneously, without sacrificing sensitivity.

2.3 Image Plane Combiner

In a previous proceeding about Silmaril,[8] we simulated the performance of both a pupil plane combiner and an image plane combiner using three telescopes. The results showed that an image plane combiner presents an advantage in terms of sensitivity. Therefore we decided to design a new image plane combiner using 3 telescopes, instead of just upgrading the CLIMB combiner which is a pupil-plane combiner, as was the plan originally.

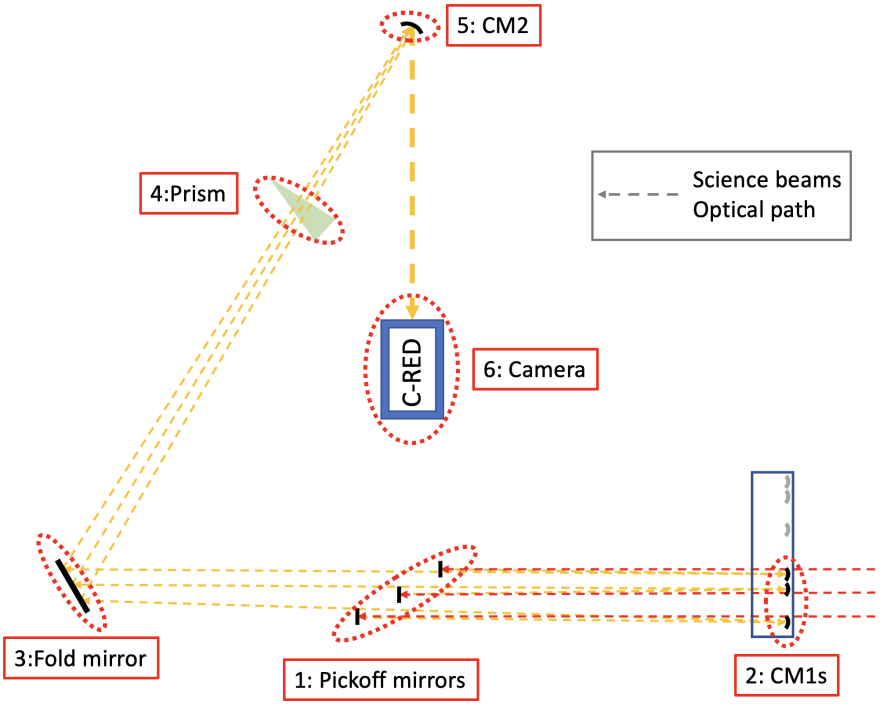

Figure 1. Scheme of the optical layout of Silmaril

2.4 Minimal Design

Each optical element in a beam combiner brings a small loss of flux coming from the telescopes, reducing the total throughput of the instrument. To obtain the best sensitivity possible, we decided to use a design limiting the number of optical elements in the beam path to get the best throughput possible.

To achieve such an objective, we use a long focal length ($\approx$ 5.4 m) cylindrical mirror (CM1) to focus the beams in the fringe directions on the detector. In the spectral direction, we use a smaller focal length (0.35 m) cylindrical mirror (CM2). Just before this short cylindrical mirror, we disperse spectrally the beams with a low resolution ($R \approx 35$) prism. This will allow us to use group delay tracking to track the fringes during observations without dispersing the light too much, limiting the loss in sensitivity.

Figure 1 shows the optical layout in the instrument lab of the CHARA Array. Because of the real estate available to us in the optical lab of the CHARA Array, and the particular long focal length design, we had to add fold mirrors at 2 different positions in the design. The first position has 3 fold mirrors (1 in Fig. 1) picking up the 3 beams that will be combined. These fold mirrors send the beams to the set of 3 cylindrical mirrors with long a focal length in the fringe direction that are disposed on top of the MIRC-X/MYSTIC instrument table, which is located next to the Silmaril table (2 in Fig. 1). The second position has a large fold mirror (3 in Fig. 1) that sends the 3 beams together through the prism (4 in Fig. 1) and on the second cylindrical mirror with a shorter focal length in the spectral direction (5 in Fig. 1). The first fold mirrors are necessary so we can position the CM1s far enough that with the combination of the second fold mirror and the CM2 acting as another fold mirror at the same time, we have enough distance to focus the beams on the camera, with the camera still fitting on the optical table (6 in Fig. 1). In addition, it allows us to set the CM1s at a height that allows the beams to travel above the optics of the other instruments already present on the Silmaril optical table (10.25 inches above the optical table instead of 6 inches for other optical elements).

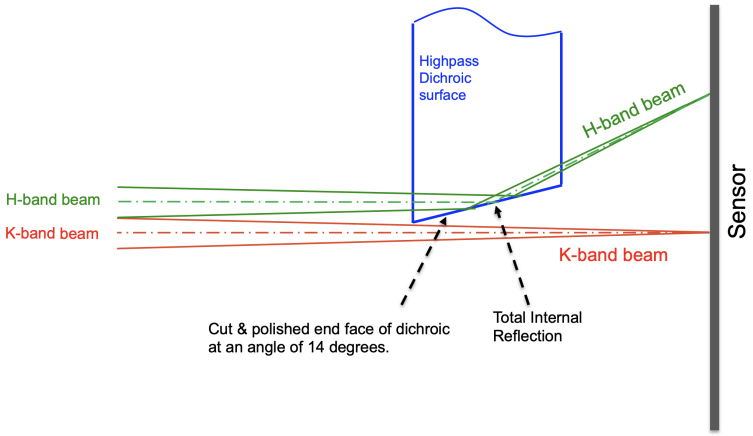

Figure 2. Scheme of the dichroic edge filter principle.

2.5 Knife-edge Filter

The possibility of observing both H- and K-band with Silmaril does not have a direct influence on the sensitivity of Silmaril, but it gives it flexibility in the science we can perform with it. To be efficient in observing H- or K-band with it, we decided to be able to observe both spectral bands at the same time, instead of having to choose which one to use with a set of different filters in front of the camera as CLASSIC/CLIMB does.

This decision comes with the difficulty of having potentially the K-band thermal photon polluting the H-band science photons, if we want the K-band science photons to reach the detector. To overcome this problem which would reduce drastically the sensitivity in the H-band, we came up with the knife-edge filter design. Half of the edge filter would let through the K-band photons from both the thermal background and the science light, while the other half lets through only the H-band photons, reducing the thermal background on this part of the detector. To do so, we presented a design for such a filter previously.[8] The main difficulties of this design were to get the filter close enough to the detector, or the transition between the 2 sides of the filter sharp enough, that the transition as seen on the detector would not pollute the H-band part of the science photons, as the separation between the H- and K-band science photons have a fixed size on the detector. This study concluded that it was too risky for the detector to move the filter closer to the detector, so the transition would need to be 100 μm sharp or better.

The procurement of a knife-edge filter with such a sharp transition in the coating was very difficult. Only one company showed in interest in trying to manufacture it, and the lead time for its fabrication was significant. Therefore, while looking for a manufacturer and to get it manufactured in the end, we decided to come up with an alternative design that would be easier to manufacture, but with uncertainties on whether it would work as designed or not.

This alternative design would use an off-the-shelf H-band filter, that would be cut in half, and the edge ground at a predetermined angle to have an internal full reflection of the H-band science photons (see Fig. 2). This design has the advantage of being easier and cheaper to manufacture, and to send the H-band further away from the transition seen by the detector between the H- and K-band parts of the detector. It means that the sharpness of the transition on the half filter does not need to be as narrow as for the first design.

As the ground edge will need to reflect the full width of the H-band, the angle of the grinding needs to be large enough, but we want to limit this angle as much as possible to avoid sending the reflected band too far. Then, as the H-band will go through the glass of the filter and not the K-band, this will add some optical length to the H-band, unmatching the focal length of the two spectral bands, making one of the bands not focused (spread) on the detector. The optical length added due to the reflection will also affect the optical path length, adding some

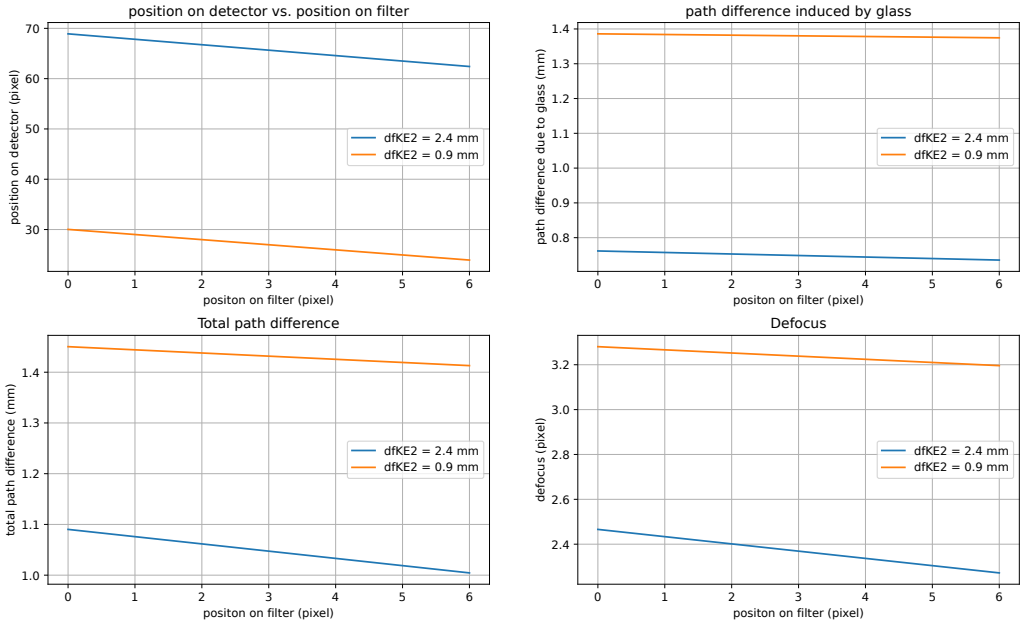

Figure 3. Results of the computation of the effect of the reflection for the H-band. Top-left: Position of the light on the detector as a function of its position if there is no reflection. Top-right: The optical path difference induced by the travel through the glass only. Bottom-left: Total optical path difference, taking into account both the one induced by the reflection and the travel through the glass of the H-band. Bottom-right: Defocus as a function of the position on the detector if no reflection. In blue, the normal distance between the end of the filter and the detected, in orange, if we get the filter closer to the detector.

path to the spectral band reflected. The full computation of these aspects can be found in a technical report available on the CHARA website*. We present in this proceeding a summary of the results.

2.5.1 Results of the simulations

The computation of the minimum angle for the ground edge gives us an angle of 11.23° for the flat filter filter and 5.11° if we use the design that gets the surface of the filter closer to the detector. The latter design has been abandoned but we still present the results of its effect in this paper. For a matter of tolerances in the manufacturing of the internal reflection edge filter, we chose to grind the edge at an angle of 12°.

Figure 3 summarizes the results. For the top-left plot, we can see that the H-band is reflected between pixels 62 and 69 away from the point of origin taken as pixel 0, where the H-band would fall on the detector without a reflection. It also means that the H-band would be spread over 7 pixels, instead of 6 without reflection, increasing slightly the spectral resolution. The top-right and bottom-left show that the path difference induced by the glass is around 7mm and between 1.0 and 1.1mm in total, meaning that the reflection induces an optical path difference of 0.3 to 0.4mm. We can conclude then that the travel through the glass is the one that dominates the difference in optical path length with twice the effect of the reflection. The bottom-right plot shows the defocus of the H-band if we focus the K-band on the detector, in pixels. The defocus is defined here as how many pixels a beam would be spread on the detector, due to the focus of the beam being reached before the detector, due to the additional optical length. We can see that for the initial filter position, the defocus would be between **2.3 and 2.5 pixels**. For the filter that would be closer to the detector, inducing a thicker filter, the defocus would be even worse, as the dominant factor adding optical length is the travel in the glass, which would be longer in

*https://www.chara.gsu.edu/files/chara_technical_reports/TR126_dichroic_edge_filter-2.pdf

this case, compared to the use of a smaller angle of reflection that reduces the amount of optical path added by the reflection. Even though the idea of getting the filter closer to the detector has been abandoned, we conclude that this solution would be worse in the case of a dichroic edge filter.

2.5.2 Final edge filter design

As mentioned previously, the knife-edge filter design has been difficult to manufacture while the internal reflection filter design has been faster and easier. Because of that and the time constraint to procure the camera, in which the filter needs to be implemented, we decided to use the internal reflection design, as at the time of the camera's final manufacturing process the knife-edge filter was still being manufactured.

The effect of this edge filter on the thermal background could then be measured and is shown in Fig. 4 and 5. In Fig. 4 we can see a separation between a high thermal background (K-band side) on the left and a low thermal

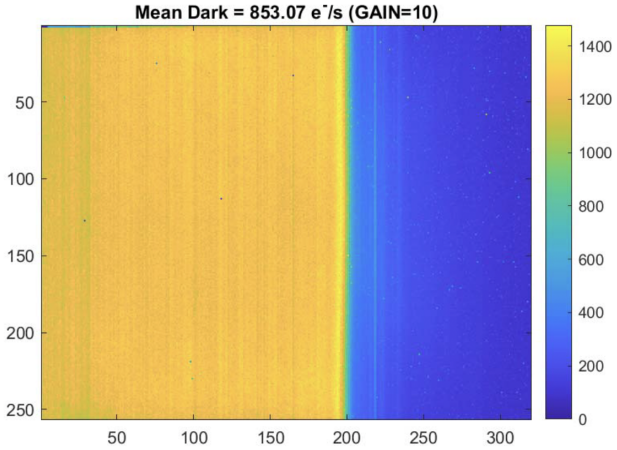

Figure 4. Thermal background measured on the detector, at room temperature, with the internal reflection edge filter installed

background (H-band side) on the right. We can also see that the transition is not positioned at the middle of the detector ($x = 160$) but further right ($x \approx 200$. This can be a problem as the H-band will be reflected about 70 pixels further from that transition position on the right, but it should still be reflected on the detector.

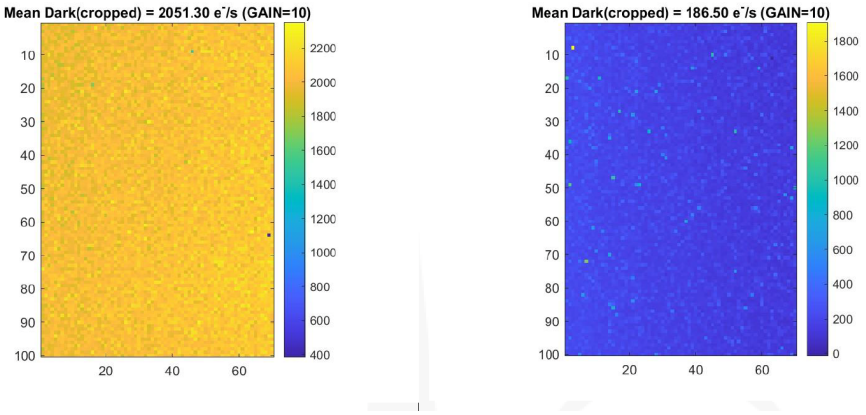

Figure 5. Thermal background measured on the detector, at room temperature, with the internal reflection edge filter installed, for each side of the detector. Left: K-band side of the detector. Right: H-band side of the detector.

In Fig. 5, we can see that the K-band part of the detector sees a thermal background of $\approx 2050 e^-/s/pix$ while the H-band sees one of $\approx 185 e^-/s/pix$. These results are in agreement with the expected thermal background these two sides should see.

After the camera was delivered at the CHARA Array, we could test if this internal reflection edge filter was working. So, we installed the camera at its dedicated place in Silmaril and used the lab source STS (Six-Telescope Simulator) that simulates flux coming from the six telescopes of the Array. We then aligned the light coming on the 3 beams used by Silmaril so that the H-band would fall on the ground part of the edge filter, and we obtained the image in figure 6. We can see on this the K-band just before the transition of the background, and

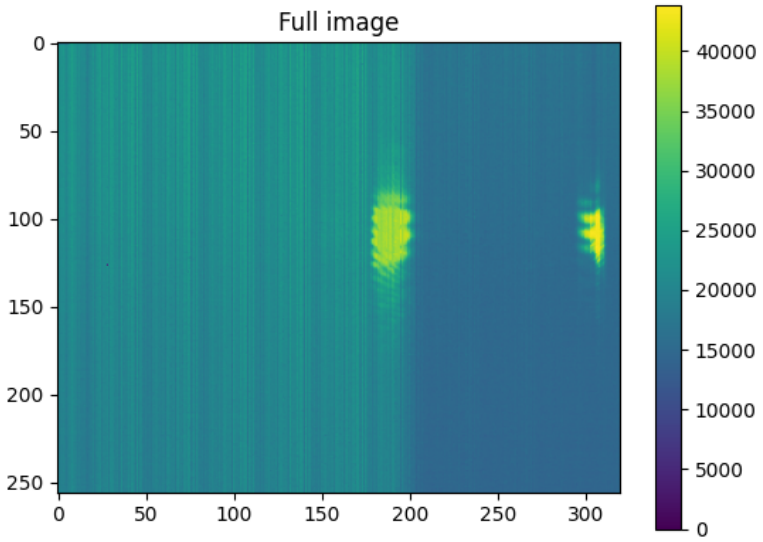

Figure 6. Laboratory fringes obtained with STS: reflected H-band fringes on the right side of the detector, K-band fringes not reflected in the middle.

the H-band projected away, close to the edge of the detector. This shows that the H-band is indeed reflected on the ground part of the edge filter away from the transition of the filter seen by the detector. Note that the camera, even though working partially as shown by those lab results, showed improper behavior once applying avalanche gain and readout mode specifically implemented to reduce the readout noise of the detector. Because of that, we had to ship back the camera rapidly to the manufacturer to fix the origin of the issue, and we could not perform on-sky observations or further tests on the performance of the internal reflection edge filter at the time this proceeding was written.

2.6 Narcissus Mirror

As you can see from the previous section, the K-band side of the detector still receives a high amount of thermal background. This will affect the SNR of the fringes measured in the spectral band. To lower this effect, it was originally planned to develop and manufacture a cryostat that would be put in front of the camera and would contain the CM2 and the prism. However, due to the design and the way the beams come to the CM2 and are reflected to the detector, a cryostat would have a difficult design. We designed an alternative solution to reduce the thermal background perceived by the detector. This alternative is called a Narcissus mirror. It consists of a spherical mirror positioned at the same distance from the detector as its radius of curvature (2 times its focal length). This mirror would have a hole in its center to let through the coming science beam (shaped to just fit the shape of the beam). The detector would then not receive thermal background photons from the surrounding elements, only the reflected thermal photon it would emit itself. With the detector in the C-RED ONE being cooled to 80K, this would drastically reduce the perceived thermal background to almost zero. This concept has not yet been tested on an astronomical instrument, but it has been also developed for the HEIMDALLR instrument currently under construction.[15]

We plan to test the efficiency of such a design once the functional C-RED ONE camera is delivered to the CHARA Array. To do so, we will use a spherical mirror without a hole in the center of it. We will place it at 2 times the focal length of the mirror from the detector. We will then compare the background measured

on the camera with and without the mirror. If this experiment shows good results in lowering the thermal background seen by the detector, we will then move forward in the procurement and manufacturing of such a mirror specifically for Silmaril's design.

3. EXPECTED ON-SKY PERFORMANCE

While we were waiting for the science camera to be shipped to the CHARA Array, we used an engineering camera to perform some on-sky performance tests. The camera we used is a C-RED 2 on loan from Gerard van Belle at Lowell Observatory. The C-RED 2 is manufactured by the same company as the C-RED ONE we are planning to use in the final stage of the combiner. Because of a higher thermal background and readout noise, the engineering camera makes Silmaril less sensitive. However, we can easily extrapolate the performance of the instrument once using the science camera when comparing these specifications. Therefore, we performed an on-sky sensitivity test. This test consisted of pointing to a list of targets ordered from the brightest to the faintest one after the other. Once on a target, we looked for fringes and tried to lock them by group-delay tracking and recording a sequence of data. Then we moved to the next target on the list, until we pointed to a target too faint to be able to detect fringes by eye therefore not being able to track the fringes and record data. On this test, we ended up being able to detect and lock fringes up to a magnitude of 4.8 in the H-band (HD 191195). As we recorded data on this star, we were able to reduce them, obtaining the SNR of the fringes we obtained at this magnitude. The SNR measured on the data was approximately 50. We can express the SNR as :

$$SNR = \frac{ENV^2}{\sqrt{EN + N_p(2 \times \sigma_R^2 + E^2\sigma_B^2)}} \tag{1}$$

where E is the exposure time in s, N is the number of photons expected in one second, V is the visibility, N_p the number of pixels, σ_R is the readout noise e^-/pix, and σ_B is the thermal background noise in $e^-/pix/s$. Most of these values are known and specified in Table 1.

Table 1. Model Beam Combiner Parameters

Parameter	C-RED 2 H	C-RED ONE H	C-RED ONE K
E	0.050	0.050	0.050
V	0.9	0.9	0.9
Pixel size (μm)	15	24	24
N_P	$7 \times 180 = 1260$	$\frac{15^2}{24^2} \times 1260/0.6$	$\frac{15^2}{24^2} \times 1260/0.6$
σ_R	30	0.96	0.96
σ_B	600	187	2051

To determine N, we fit a linear model to data collected during the observations (Fig. 7). We obtain:

$$N = 6.0 \times 10^7 10^{-M/2.5} \tag{2}$$

where M is the magnitude of the observed target. This number is derived from the C-RED 2 camera that has a cutoff wavelength at 1.7 μm. This represents only 60% of the full H-band. The C-RED ONE camera will have both the full H-band and the K-band. Each of these will get 1/0.6 more flux over 1/0.6 more pixels than the C-RED 2. We compute the total SNR as a combination of both H- and K-band SNR:

$$SNR_1 = \sqrt{SNR_H^2 + SNR_K^2} \tag{3}$$

This gives us an SNR of $\approx$ 50 for a magnitude of 4.5 for the C-RED 2, which is consistent with our on-sky measurement.

We plot the resulting comparison between both cameras in Figure 8. In this figure, we can see that the C-RED 2 camera should be able to reach an SNR of 5 for a target with a magnitude of 7.03, therefore the C-RED

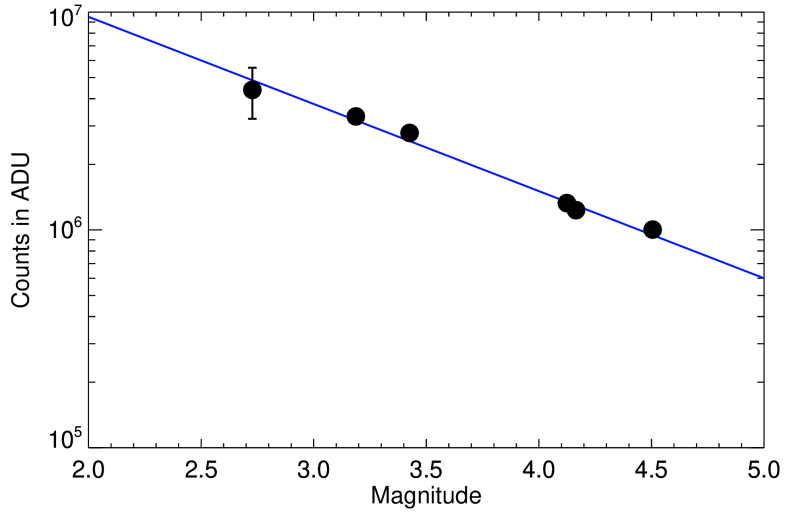

Figure 7. Recorded flux as a function of the target's magnitude.

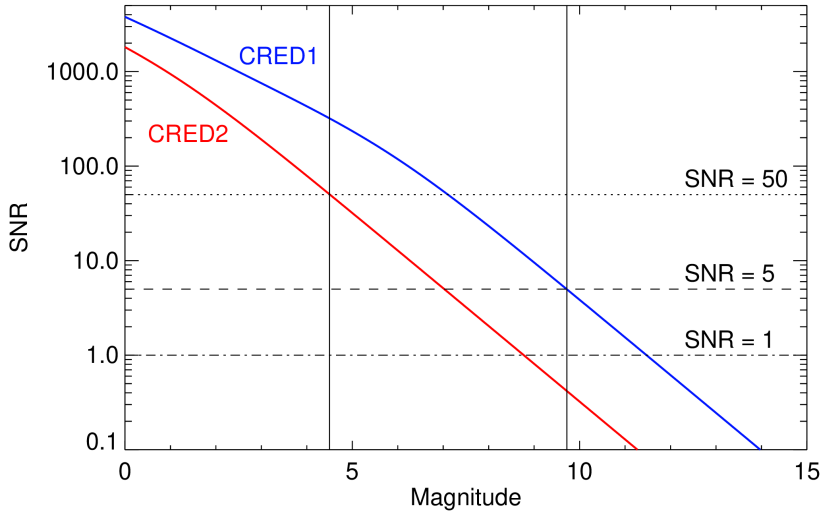

Figure 8. Modeled SNR as a function of the target's magnitude.

ONE should reach the same SNR for a target's magnitude of 9.7. This SNR of 5 is the one reached typically by the MIRC-X[4] when tracking fringes on a faint star and gives us a good estimate of what Silmaril should be able to track easily. This estimation of limiting magnitude is based on a single night of observation with no further optimization, but it is in agreement with the estimated limiting magnitude goal for the project and the further simulation performed in the earliest stage of the project.[8] When optimized for really faint observations (less pixel read, longer exposure times, adapted observing strategy), we can record fringes close to an SNR of 1. We can see in Figure 8 that the C-RED ONE camera should be able to reach this SNR for a magnitude of 11.47. Therefore we expect to be able to observe targets fainter than 10.5 in magnitude.

4. CONCLUSIONS

First, we were not sure if the design we chose for the edge filter would work as intended. After some tests with lab light, we can conclude that the principle of an internal reflection of the H-band on the edge filter is working.

We still need to perform more tests to confirm if it works perfectly as intended or if there is some effect reducing its efficiency.

Then, the first tests performed on-sky with an engineering camera allowed us to estimate the performance we should be able to reach with the science camera. We should be able to track on target with a magnitude of at least 10.5, which validates the previous simulations of the limiting magnitude of Silmaril. It also reaches the goal aimed for this project to improve the limiting magnitude achievable at the CHARA Array by two magnitudes, opening the AGN science case particularly.

ACKNOWLEDGMENTS

The SILMARIL project at the CHARA Array is supported by the National Science Foundation under Grant No. AST-1909858. Institutional support has been provided from the GSU College of Arts and Sciences and the GSU Office of the Vice President for Research and Economic Development.

REFERENCES

[1] ten Brummelaar, T. A., Gies, D. G., McAlister, H. A., Ridgway, S. T., Sturmann, J., Sturmann, L., Schaefer, G. H., Turner, N. H., Farrington, C. D., Scott, N. J., Monnier, J. D., and Ireland, M. J., "An update on the chara array," *Proc.SPIE* **9907**, 9907 – 9907 – 7 (2016).

[2] Beckmann, U., Connot, C., Heininger, M., Hofmann, K.-H., Nußbaum, E., Schertl, D., Solscheid, W., ten Brummelaar, T., Turner, N., and Weigelt, G., "A low-noise HAWAII detector system and new cold optics for the CLASSIC/CLIMB beam combiner instrument of the CHARA array," in [*Optical and Infrared Interferometry IV*], *Proc. SPIE* **9146**, 91461W (7 2014).

[3] GRAVITY collaboration, Abuter, R., Accardo, M., Amorim, A., Anugu, N., Ávila, G., Azouaoui, N., Benisty, M., Berger, J. P., Blind, N., Bonnet, H., Bourget, P., Brandner, W., Brast, R., Buron, A., Burtscher, L., Cassaing, F., Chapron, F., Choquet, É., Clénet, Y., Collin, C., Coudé Du Foresto, V., de Wit, W., de Zeeuw, P. T., Deen, C., Delplancke-Ströbele, F., Dembet, R., Derie, F., Dexter, J., Duvert, G., Ebert, M., Eckart, A., Eisenhauer, F., Esselborn, M., Fédou, P., Finger, G., Garcia, P., Garcia Dabo, C. E., Garcia Lopez, R., Gendron, E., Genzel, R., Gillessen, S., Gonte, F., Gordo, P., Grould, M., Grözinger, U., Guieu, S., Haguenauer, P., Hans, O., Haubois, X., Haug, M., Haussmann, F., Henning, T., Hippler, S., Horrobin, M., Huber, A., Hubert, Z., Hubin, N., Hummel, C. A., Jakob, G., Janssen, A., Jochum, L., Jocou, L., Kaufer, A., Kellner, S., Kendrew, S., Kern, L., Kervella, P., Kiekebusch, M., Klein, R., Kok, Y., Kolb, J., Kulas, M., Lacour, S., Lapeyrère, V., Lazareff, B., Le Bouquin, J. B., Lèna, P., Lenzen, R., Lévêque, S., Lippa, M., Magnard, Y., Mehrgan, L., Mellein, M., Mérand, A., Moreno-Ventas, J., Moulin, T., Müller, E., Müller, F., Neumann, U., Oberti, S., Ott, T., Pallanca, L., Panduro, J., Pasquini, L., Paumard, T., Percheron, I., Perraut, K., Perrin, G., Pflüger, A., Pfuhl, O., Phan Duc, T., Plewa, P. M., Popovic, D., Rabien, S., Ramírez, A., Ramos, J., Rau, C., Riquelme, M., Rohloff, R. R., Rousset, G., Sanchez- Bermudez, J., Scheithauer, S., Schöller, M., Schuhler, N., Spyromilio, J., Straubmeier, C., Sturm, E., Suarez, M., Tristram, K. R. W., Ventura, N., Vincent, F., Waisberg, I., Wank, I., Weber, J., Wieprecht, E., Wiest, M., Wiezorrek, E., Wittkowski, M., Woillez, J., Wolff, B., Yazici, S., Ziegler, D., and Zins, G., "First light for GRAVITY: Phase referencing optical interferometry for the Very Large Telescope Interferometer," *A&A* **602**, A94 (6 2017).

[4] Kraus, S., Monnier, J. D., Anugu, N., Bouquin, J.-B. L., Davies, C. L., Ennis, J., Labdon, A., Lanthermann, C., Setterholm, B., and ten Brummelaar, T., "The mirc-x 6-telescope imager: key science drivers, instrument design and operation," *Proc.SPIE* **10701**, 10701 – 10701 – 13 (2018).

[5] Anugu, N., Le Bouquin, J.-B., Monnier, J. D., Kraus, S., Setterholm, B. R., Labdon, A., Davies, C. L., Lanthermann, C., Gardner, T., Ennis, J., Johnson, K. J. C., Ten Brummelaar, T., Schaefer, G., and Sturmann, J., "MIRC-X: A Highly Sensitive Six-telescope Interferometric Imager at the CHARA Array," *AJ* **160**, 158 (Oct. 2020).

[6] Monnier, J. D., Bouquin, J.-B. L., Anugu, N., Kraus, S., Setterholm, B. R., Ennis, J., Lanthermann, C., Jocou, L., and ten Brummelaar, T., "Mystic: Michigan young star imager at chara," *Proc.SPIE* **10701**, 10701 – 10701 – 19 (2018).

[7] Setterholm, B. R., Monnier, J. D., Le Bouquin, J.-B., Anugu, N., Ennis, J., Jocou, L., Ibrahim, N., Kraus, S., Anderson, M. D., Chhabra, S., Codron, I., Farrington, C. D., Flores, B., Gardner, T., Gutierrez, M., Lanthermann, C., Majoinen, O. W., Mortimer, D. J., Schaefer, G., Scott, N. J., ten Brummelaar, T., and Vargas, N. L., "MYSTIC: a high angular resolution K-band imager at CHARA," *Journal of Astronomical Telescopes, Instruments, and Systems* **9**, 025006 (Apr. 2023).

[8] Lanthermann, C., ten Brummelaar, T., Tuthill, P., Martinod, M.-A., Ligon, E., Gies, D., Schaefer, G., and Anderson, M., "Design of the new CHARA instrument SILMARIL: pushing for the sensitivity of a 3-beam combiner in the H- and K-bands," **12183**, 121830N (Aug. 2022).

[9] Finger, G., Baker, I., Dorn, R., Eschbaumer, S., Ives, D., Mehrgan, L., Meyer, M., and Stegmeier, J., "Development of high-speed, low-noise nir hgcdte avalanche photodiode arrays for adaptive optics and interferometry," *Proc.SPIE* **7742**, 7742 – 7742 – 14 (2010).

[10] Finger, G., Baker, I., Alvarez, D., Ives, D., Mehrgan, L., Meyer, M., Stegmeier, J., Thorne, P., and Weller, H. J., "Evaluation and optimization of nir hgcdte avalanche photodiode arrays for adaptive optics and interferometry," *Proc.SPIE* **8453**, 8453 – 8453 – 16 (2012).

[11] Finger, G., Baker, I., Alvarez, D., Ives, D., Mehrgan, L., Meyer, M., Stegmeier, J., and Weller, H. J., "Saphira detector for infrared wavefront sensing," **9148** (2014).

[12] Finger, G., Baker, I., Alvarez, D., Dupuy, C., Ives, D., Meyer, M., Mehrgan, L., Stegmeier, J., and Weller, H. J., "Sub-electron read noise and millisecond full-frame readout with the near infrared eapd array saphira," *Proc.SPIE* **9909**, 9909 – 9909 – 20 (2016).

[13] Greffe, T., Feautrier, P., Gach, J.-L., Stadler, E., Clop, F., Lemarchand, S., Boutolleau, D., and Baker, I., "C-red one : the infrared camera using the saphira e-apd detector," *Proc.SPIE* **9907**, 9907 – 9907 – 9 (2016).

[14] Anugu, N., ten Brummelaar, T., Lanthermann, C., Tuthill, P., Ligon, E., Gies, D., and Schaefer, G., "CHARA/Silmaril Instrument Software and Data Reduction Pipeline: Characterization of the Instrument in the Lab and On-Sky," in [*Optical and Infrared Interferometry and Imaging IX*], Mérand, A., Sallum, S., and Sanchez-Bermudez, J., eds., *Society of Photo-Optical Instrumentation Engineers (SPIE) Conference Series* **13095-46** (Aug. 2024).

[15] Taras, A. K., Robertson, J. G., Allouche, F., Courtney-Barrer, B., Carter, J., Crous, F., Cvetojevic, N., Ireland, M., Lagarde, S., Martinache, F., McGinness, G., N'Diaye, M., Robbe-Dubois, S., and Tuthill, P., "Heimdallr, Baldr, and Solarstein: designing the next generation of VLTI instruments in the Asgard suite," *Appl. Opt.* **63**, D41 (May 2024).